Point Mutations in αbENaC Regulate Channel Gating, Ion Selectivity, and Sensitivity to Amiloride

Catherine M. Fuller, Bakhram K. Berdiev, Vadim G. Shlyonsky, Iskander I. Ismailov, and Dale J. Benos
Department of Physiology and Biophysics, University of Alabama at Birmingham, Birmingham, Alabama 35294 USA

ABSTRACT We have generated two site-directed mutants, K504E and K515E, in the α subunit of an amiloride-sensitive bovine epithelial Na^+ channel, αbENaC. The region in which these mutations lie is in the large extracellular loop immediately before the second membrane-spanning domain (M2) of the protein. We have found that when membrane vesicles prepared from *Xenopus* oocytes expressing either K504E or K515E αbENaC are incorporated into planar lipid bilayers, the gating pattern, cation selectivity, and amiloride sensitivity of the resultant channel are all altered as compared to the wild-type protein. The mutated channels exhibit either a reduction or a complete lack of its characteristic burst-type behavior, significantly reduced Na^+:K^+ selectivity, and an approximately 10-fold decrease in the apparent inhibitory equilibrium dissociation constant (K_i) for amiloride. Single-channel conductance for Na^+ was not affected by either mutation. On the other hand, both K504E and K515E αbENaC mutants were significantly more permeable to K^+, as compared to wild type. These observations identify a lysine-rich region between amino acid residues 495 and 516 of αbENaC as being important to the regulation of fundamental channel properties.

INTRODUCTION

The ENaCs are a recently identified family of amiloride-sensitive Na^+ channels. Originally cloned from epithelial tissues (rat colon, human lung; Canessa et al., 1993; Linguelia et al., 1993; McDonald et al., 1994; Voilley et al., 1994), other related members of the family mediate mechanosensitivity in the nematode *Caenorhabditis elegans* and have been found in neural tissue in both humans and gastropods (Price et al., 1996; Linguelia et al., 1995; Driscoll and Chalfie, 1991; Chalfie and Wolinsky, 1990). The epithelial ENaCs are composed of three subunits, termed α, β, and γ, and although the exact stoichiometry is not known, all three subunits are required to observe maximum amiloride-sensitive current in the *Xenopus* oocyte heterologous expression system (Canessa et al., 1994b; McDonald et al., 1995; Voilley et al., 1995). However, the α subunit can function as an amiloride-sensitive Na^+ channel in the absence of the β and γ subunits, both when expressed in *Xenopus* oocytes or when reconstituted into planar lipid bilayers after in vitro translation (Canessa et al., 1993; Fuller et al., 1995; Ismailov et al., 1996a). The bovine α isoform, αbENaC, has been recently cloned from the bovine renal papilla (Fuller et al., 1995). When expressed in *Xenopus* oocytes, this isoform produces amiloride-sensitive Na^+ currents both when expressed alone and in conjunction with β and γrENaC. When vesicles from αbENaC-expressing oocytes are fused to planar lipid bilayers, single sodium-selective, amiloride-sensitive 39-pS channels are clearly observed (Awayda et al., 1995; Fuller et al., 1996). Hydrophobicity plots predict that this isoform has a topological organization nearly identical to that found in the other ENaC isoforms, namely, two membrane-spanning domains, termed M1 and M2, separated by a large (428 amino acid) loop that is external to the cell membrane (Renard et al., 1994; Canessa et al., 1994a; Snyder et al., 1994).

Although ENaC subunits have been identified in several species, little is currently known concerning the sequence/function relations of the protein. Using site-directed mutagenesis and antiidiotypic amiloride antibodies, Ismailov et al. (manuscript submitted for publication) have identified a putative amiloride binding motif in the rat α subunit between residues 278 and 283 in the extracellular loop, consistent with an extracellular site of action of the drug. Insertion of a premature stop codon at Arg 564 in the human βENaC subunit results in a channel with a dramatically increased open probability and/or more channels trafficked to the cell surface (Shimkets et al., 1994). Similar observations have been made for the human γENaC subunit (Hansson et al., 1995a). Truncations as well as point mutations in a consensus PPPXY sequence in either the β or γENaC C terminal regions (as occurs in the hypertensive condition known as Liddle's syndrome) result in a nearly constitutively open channel (Ismailov et al., 1996b), and an increase in whole-cell current when the constructs are expressed in *Xenopus* oocytes (Hansson et al., 1995b; Schild et al., 1996), suggesting that this region is important for channel gating and/or channel trafficking to the cell membrane (Rotin et al., 1994; Staub et al., 1996; McDonald and Welsh, 1995). A point mutation (as well as frameshift mutations) in the N terminus of the αENaC subunit have also been associated with pseudohypoaldosteronism, a condition complementary to Liddle's syndrome (Chang et al., 1996). We have previously shown that synthetic peptides correspond-

Received for publication 18 August 1996 and in final form 31 December 1996.

Address reprint requests to Dr. C. M. Fuller, Department of Physiology and Biophysics, University of Alabama at Birmingham, BHSB 735, 1918 University Boulevard, University Station, Birmingham AL 35294-0005. Tel.: 205-934-6085; Fax: 205-934-2377; E-mail: fuller@phybio.bhs.uab.edu.

0006-3495/97/04/1622/11 $2.00

ing to the extreme C termini of the human β and γ ENaC subunits can act as blocking particles for the channel pore (Ismailov et al., 1996b; Bubien et al., 1996), in a manner analogous to that first described for the Shaker K^+ channels (Hoshi et al., 1990; Zagotta et al., 1990). In addition, the extreme C terminal of αbENaC modifies the unique gating behavior of this bovine ENaC isoform (Fuller et al., 1996).

In the present study, we tested the hypothesis that a region in the extracellular loop of αbENaC, predicted to lie immediately before the second hydrophobic M2 domain and therefore forming part of the outer face of the putative pore region, was involved in the regulation of αbENaC channel properties, such as gating, conductance, and ion selectivity. This region, comprising residues 495–516, consists of a repeating lysine motif (IKNKRDGVAKLNIFFKELNYKS) that is highly conserved between all of the mammalian αENaC subunits identified so far. In many cation channels, notably the Ca^{2+}-activated K^+ channel (MacKinnon and Miller, 1989), batrachotoxin-sensitive Na^+ channel (Worley et al., 1986), voltage-dependent Shaker K^+ channels (Perozo et al., 1994), and the nicotinic ACh receptor (Imoto et al., 1988; Konno et al., 1991), the presence of fixed charges influences channel properties such as conductance and gating currents. A similar sequence in the S4 region of the Shaker K^+ channels that comprises a repeating arginine motif seems to form part of the voltage sensor of the channel, and therefore has a critical role in determining channel gating (Perozo et al., 1994). Using site-directed mutagenesis, we have reversed the fixed positive charge on lysines 504 and 515 to a fixed negative charge by mutating lysine to glutamic acid. We now report that these mutations result in dramatic changes in some fundamental characteristics of αbENaC function, such as ion selectivity, gating kinetics, and sensitivity to amiloride.

MATERIALS AND METHODS

Materials

Molecular reagents were obtained from Promega (Madison WI), New England Biolabs (Beverly, MA), Amersham (Arlington Heights, IL), or Stratagene (La Jolla, CA). Female *Xenopus laevis* were obtained from *Xenopus* I (Ann Arbor, MI). Radioactive [^{35}S]methionine and [^{32}P]dATP were obtained from Dupont/NEN. Lipids for planar bilayer experiments were purchased from Avanti Polar Lipids (Birmingham, AL). All other reagents were obtained either from Sigma, BioRad, or Fisher (Pittsburgh, PA).

METHODS

Site-directed mutagenesis

Site-directed mutagenesis of K504 and K515 was achieved by use of the ExSite PCR-based mutagenesis kit from Stratagene. We synthesized two pairs of primers, oriented in opposite directions, according to the manufacturer's instructions. These primer pairs were homologous to either the sense or antisense strands of αbENaC, with the exception of a single base mismatch at the site of the mutation. This mismatch resulted in the exchange of lysine for glutamic acid at the relevant position. The αbENaC insert was cloned into a modified pGEM 11 vector, containing the 5′ and 3′ untranslated regions of *Xenopus* β globin, 5′ and 3′ to the insert, as previously described (Fuller et al., 1995). This double-stranded plasmid acted as a template for the polymerase chain reaction (PCR). The two primer sets used were K504E sense, 5′-CTCAACATCTTCTTCAAG-GAGCT-3′ and K504E antisense, 5′-TTCGGCAACTCCATCCCTTT-TGT-3′; K515E sense, 5′-TCTAATTCTGAGTCTCCCTCAGTC-3′ and K515E antisense, 5′-TTCGTAGTTCAGCTCCTTGAAG-3′. The PCR cycle profile was 94°C, 4 min, 54°C, 2 min, 72°C, 2 min for one cycle; 94°C, 1 min, 56°C, 2 min, 72°C, 1 min, for 12 cycles, and a final extend step at 72°C for 5 min. The PCR reaction was also modified by the addition of 4% formamide. After PCR, the reaction was digested with *Dpn*I to remove the parental template and polished with *pfu* polymerase (Stratagene) for 30 min at 72°C. The final PCR product (approximately 5.3 kb) was then ligated with T4 ligase and transformed into XLI-Blue Supercompetent cells. Transformants were picked and sequenced to identify those containing the appropriate mutation. Plasmids with inserts containing the mutation of interest were linearized with *Bam*HI and in vitro transcribed with SP6 polymerase, in the presence of a methylguanosine cap analog, $m^7G(5')ppp(5')G$. The integrity of the resultant cRNAs was checked by electrophoresis through 1% denaturing agarose formaldehyde gels, and assessed for translation competency by in vitro translation with [^{35}S]L-methionine, using micrococcal nuclease-treated rabbit reticulocyte lysate (Promega). The respective cRNAs were then used for injection into *Xenopus* oocytes.

Oocyte injection and planar lipid bilayer recording

Oocytes were defolliculated in OR-2 medium (in mM: 82.5 NaCl, 2.4 KCl, 5 $MgCl_2$, 5 HEPES, pH 7.4), containing 1 mg/ml type 1A collagenase (320 units/mg; Sigma), for 2 h with one solution change, as previously described (Fuller et al., 1995; Cunningham et al., 1995). Stage V/VI oocytes were selected and maintained for 24 h in 0.5× L-15 medium containing 15 mM HEPES and 2% of a 10,000 units/ml solution of penicillin/streptomycin. Oocytes were injected with either 50 nl nuclease-free water or 50 nl water + 25 ng of the appropriate cRNA. After a further 24–48 h, membrane vesicles were prepared from the injected oocytes and frozen at −80°C for subsequent fusion to the lipid bilayer for physiological recording as described previously (Cunningham et al., 1995; Awayda et al., 1995; Perez et al., 1994). Planar bilayer membranes were composed of a mixture of diphytanoyl phosphatidylethanolamine/diphytanoyl phosphatidylserine/oxidized cholesterol (20 mg/ml) in a 2:1:2 (w/w/w) ratio; they were bathed with symmetrical solutions of 100 mM NaCl and 10 mM 3-(*N*-morpholino)propanesulfonic acid (pH 7.5). Records were low-pass-filtered at 300 Hz using an 8-pole Bessel filter, before data acquisition with a Digidata 1200 interface (Axon Instruments, Foster City, CA) at 25 Hz and 1000 Hz to represent 20 min and 10 s of channel activity, respectively. Time-expanded records were subsequently filtered digitally at 100 Hz using pCLAMP software (Axon Instruments). Data analysis was as described previously (Ismailov et al., 1996a). Analysis of steady-state single-channel data was performed by using the Michaelis-Menten equation, rewritten for conductance as follows:

$$g = g_m \frac{[S]}{K_m + [S]}, \quad (1)$$

where g is the single-channel conductance at ion concentration [S], g_m is the maximum conductance, and K_m is the apparent dissociation constant of Na^+ (Lakshminarayanaiah, 1984).

RESULTS

Gating properties of K504E and K515E αbENaC

We have previously shown that wild-type αbENaC exhibits a unique gating pattern, characterized by periods of channel quiescence interspersed with bursts of channel activity

(Awayda et al., 1995; Fuller et al., 1996). Under control conditions, the gating of αbENaC is also characterized by a single-step transition to 39 pS, in contrast to αrENaC (the prototypical ENaC isoform originally cloned from the rat distal colon), which does not exhibit this burst-type behavior and exhibits predominantly a 13-pS open-state conductance with frequent single-step transitions of 26–39 pS (Ismailov et al., 1996a). As shown in Fig. 1, mutation of the lysine residues at position 504 or 515 to glutamic acid in αbENaC had no effect on single-channel conductance, which was still manifest as a single-step transition of 39 pS.

However, a change in the gating pattern of αbENaC was observed in both the K515E and K504E αbENaC mutants. Typically, wild-type αbENaC exhibited three or four quiescent periods of 3–7 min duration within 30 min of continuous recording. In the case of K515E, the bursts of channel activity were more frequent as compared to the wild-type control, whereas in the K504E mutant there was a further, more dramatic shift in gating, such that the channel exhibited frequent rapid transitions between open and closed states. These changes in the characteristic pattern of channel gating were dependent on the $[Na^+]$ of the bilayer bathing solution. Plots of channel conductance versus $[Na^+]$ saturated with K_m values of 42.9 ± 3.9 mM (n = 6), 40.7 ± 5.9 mM (n = 4), and 39.5 ± 3.9 mM (n = 7) for wild-type, K515E, and K504E αbENaC, respectively, as determined by fitting the experimental data to first-order Michaelis-Menten kinetics (Eq. 1, Fig. 2). The calculated g_{max} values were 58.8 ± 1.8 pS, 58.2 ± 1.5 pS, and 58.7 ± 1.5 pS for wild-type, K515E, and K504E αbENaC, respectively. The kinetic parameters of wild-type and mutant αbENaC gating at different $[Na^+]$ are shown in Table 1. K504E αbENaC

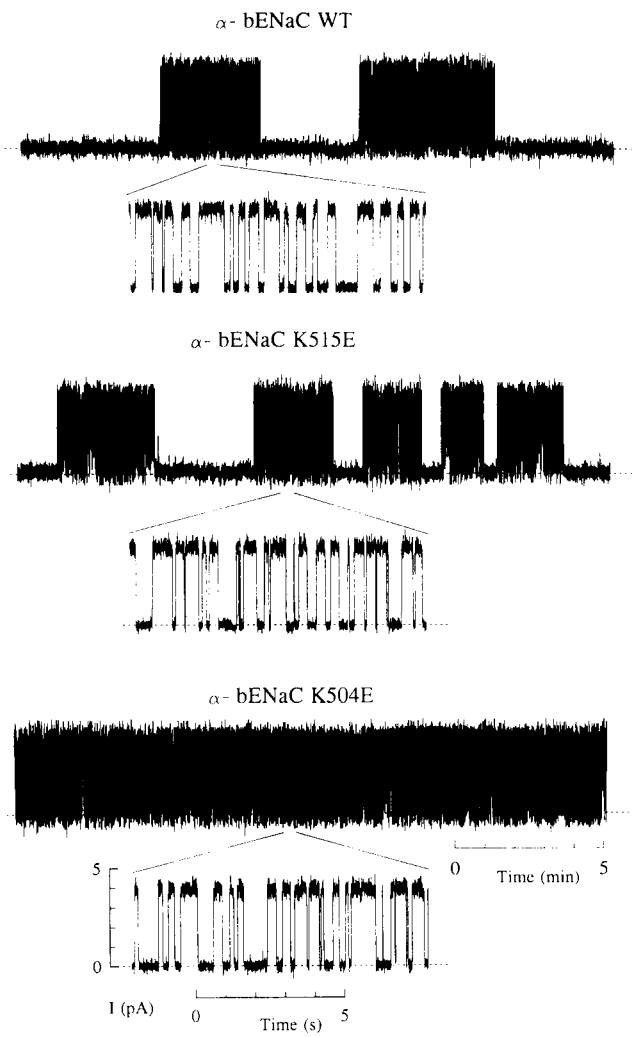

FIGURE 1 Single-channel records of wild-type (WT) and mutated (K515E and K504E) αbENaC. The cRNAs for each construct were injected and expressed in *Xenopus* oocytes as described. Oocyte vesicles were then fused to the planar lipid bilayer for electrophysiological recording. Wild-type αbENaC exhibited single-step transitions of 39 pS and a pronounced bursting pattern of activity. In K515E and K504E αbENaC, the interval between bursts was reduced such that in K504E αbENaC, the channel was continuously active. However, neither mutant exhibited any change in single-channel conductance as compared to the wild-type channel. Each record is representative of at least eight separate experiments. The holding potential was +100 mV. Records were low-pass-filtered at 300 Hz, using an 8-pole Bessel filter before data acquisition, with a Digidata 1200 interface at 25 Hz and 1000 Hz to represent 20 min and 10 s of channel activity, respectively. Time-expanded records were subsequently filtered digitally at 100 Hz using pCLAMP software. Dashed lines represent zero current.

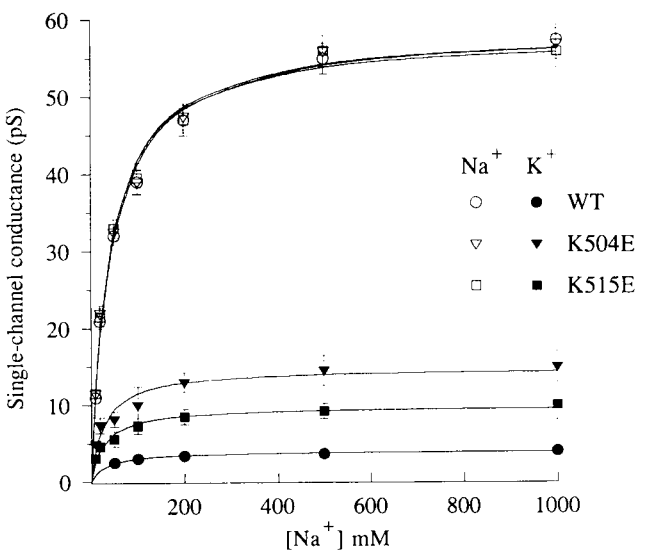

FIGURE 2 Ion concentration dependence of αbENaC chord conductance. Data points in each plot represent mean single-channel conductance of WT, K515E, and K504E αbENaC ± 1 SD. The plots of channel conductance versus $[Na^+]$ (○, ▽, □), saturated with K_m of 42.9 ± 3.9 mM (n = 6), 40.7 ± 5.9 mM (n = 4), and 39.5 ± 3.9 mM (n = 7) for WT, K515E, and K504E αbENaC, respectively, as determined by fitting the experimental data to first-order Michaelis-Menten kinetics (Eq. 1). The g_{max} values obtained from these fits were 58.8 ± 1.8 pS, 58.2 ± 1.5 pS, and 58.7 ± 1.5 pS, for WT, K515E, and K504E αbENaC, respectively. Both wild-type and mutant αbENaC channels also showed saturation of single-channel conductance for K^+ (●, ▼, ■), although they exhibited different maxima. The g_{max} values were 4.1 ± 1.1, 10.9 ± 1.1, and 15.2 ± 2.2 pS for wild-type, K515E, and K504E αbENaC, respectively, as determined by fitting the experimental data to the first-order Michealis-Menten equation (Eq. 1).

TABLE 1 Duration of burst and quiescent periods for wild-type (WT), K515E, and K504E αbENaC

	WT					K515E					K504E				
$[Na^+]$ (mM)	τ_{burst} (s)	$\tau_{quiescent}$ (s)	τ_c (ms)	τ_o (ms)	N	τ_{burst} (s)	$\tau_{quiescent}$ (s)	τ_c (ms)	τ_o (ms)	N	τ_{burst} (s)	$\tau_{quiescent}$ (s)	τ_c (ms)	τ_o (ms)	N
50	191 ± 49	398 ± 146	274 ± 31	260 ± 29	5	121 ± 33	153 ± 41	263 ± 25	270 ± 29	4	Const.	None	258 ± 32	256 ± 37	5
100	246 ± 128	367 ± 175	224 ± 27	307 ± 35	9	156 ± 36	126 ± 48	241 ± 27	281 ± 31	8	Const.	None	236 ± 25	266 ± 29	11
500	303 ± 125	292 ± 143	144 ± 27	315 ± 38	5	198 ± 61	104 ± 35	119 ± 40	302 ± 38	4	Const.	None	92 ± 25	287 ± 41	5
1000	340 ± 167	247 ± 110	77 ± 25	344 ± 42	5	248 ± 95	72 ± 19	81 ± 23	322 ± 29	4	Const.	None	75 ± 21	318 ± 31	5

The open and closed time constants (τ_o and τ_c) for channel opening within each burst period as calculated from the appropriate dwell time histograms are also shown. τ_{burst}, burst duration; $\tau_{quiescent}$, quiescent period duration; τ_c, closed time within burst; τ_o, open time within burst; Const., constitutively active; None, none observed.

exhibited no evidence of burst-type behavior in over 60 min of continuous recording, reminiscent of the gating behavior of αrENaC. The overall open probability (P_o) of the mutants at 100 mM symmetrical Na^+ was correspondingly increased from 0.19 ± 0.03 (n = 9) for wild-type αbENaC to 0.32 ± 0.04 (n = 8) and 0.55 ± 0.05 (n = 7) for K515E and K504E αbENaC, respectively. At 1 M Na^+ these values became 0.46 ± 0.07 (n = 5) for wild-type αbENaC, 0.61 ± 0.08 (n = 4) for K515E αbENaC, and 0.81 ± 0.09 (n = 5) for K504E αbENaC, respectively. However, the open probability of the wild-type channel within the burst was not different from that for either mutant channel studied under the same conditions. Moreover, no effect of charge mutations on the chord conductance of αbENaC was found over a ±120 mV potential range when studied at three different Na^+ concentrations (Fig. 3).

Ion selectivity of K504E and K515E αbENaC

Both K504E and K515E αbENaC channels exhibited linear single-channel *I/V* relationships in symmetrical 100 mM NaCl solutions, with slope conductances essentially indistinguishable from that of wild-type αbENaC (Fig. 4 *A*). However, both mutations severely compromised channel selectivity for Na^+ over K^+. Under 100 mM biionic conditions, the permeability ratio (P_{Na}:P_K) was approximately 10:1 for wild-type αbENaC. This ratio fell to 2:1 and 3:1 for K504E and K515E αbENaC, respectively, as calculated from the reversal potentials measured under biionic conditions (Fig. 4 *B*). As we observed no change in the single-channel Na^+ conductance of the mutant channels at any $[Na^+]$, this finding suggests that the introduced mutations cause either an increase in g_{K^+} of the channel or an increase in the affinity of the channel for K^+. This possibility was tested by studying the K^+ concentration dependence of single-channel conductance of wild-type and mutant αbENaC (Fig. 2). As was observed for Na^+ solutions, both wild-type and mutant αbENaC channels showed saturation of single-channel conductance for K^+, although they exhibited different maxima. These values were 4.1 ± 1.1, 10.9 ± 1.1, and 15.2 ± 2.2 pS for wild-type, K515E, and K504E αbENaC, respectively, as determined by fitting the experi-

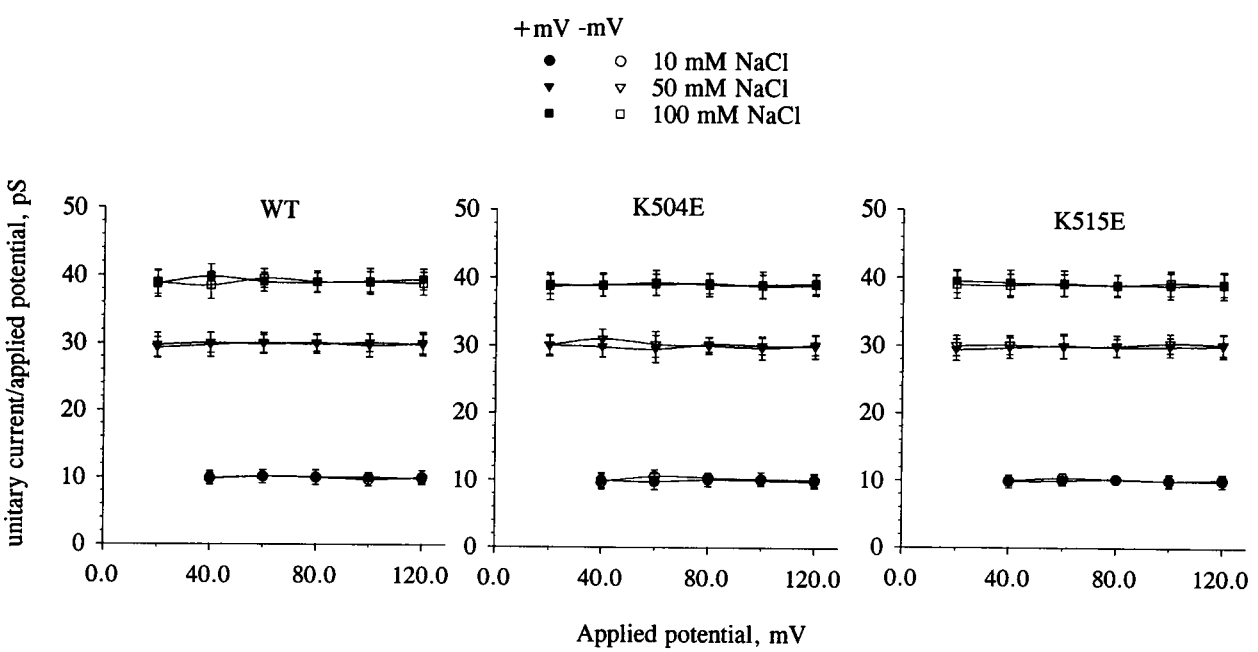

FIGURE 3 Wild-type and mutant αbENaC Na^+ conductance is voltage independent. Data points in each plot represent mean single-channel conductances of WT (n = 4), K515E (n = 3), and K504E αbENaC (n = 5) ± 1 SD.

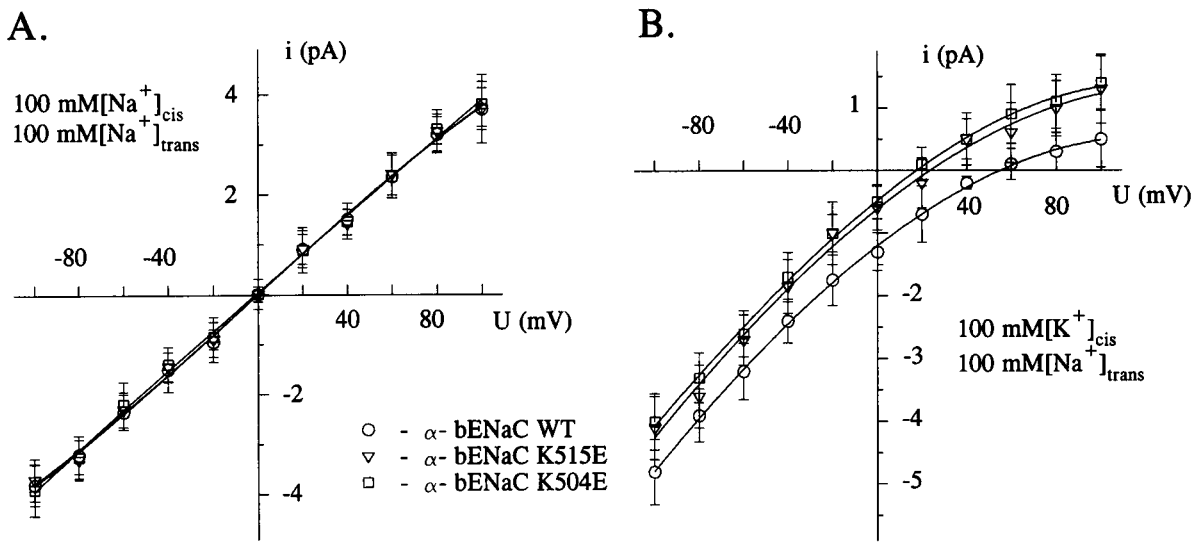

FIGURE 4 Current-voltage relationships and ion selectivity of wild-type and mutated αbENaC. Both wild-type and mutated channels exhibited a linear *I/V* relationship in symmetrical 100 mM NaCl, with slope conductances essentially indistinguishable from that of wild-type αbENaC. The ion selectivity of wild-type and mutant ENaC isoforms was determined under biionic conditions, with 100 mM Na^+ in the *trans* compartment and 100 mM K^+ in the *cis* chamber. In all experiments, bathing solutions were buffered to pH 7.5 with 10 mM 3-(*N*-morpholino)propanesulfonic acid/Tris. Values are the mean ± SD for four to seven experiments at each voltage, as calculated from the events amplitude histogram analysis performed by pCLAMP software. Histogram analysis was performed on continuous single-channel records of at least 15 min duration, filtered at 100 Hz using an 8-pole Bessel filter before acquisition. Data were sampled at 1000 Hz using a Digidata 1200 interface. The events lists were generated by pCLAMP software with a 50% amplitude detection threshold and a 5-ms event duration threshold. The calculated permeability ratio (P_{Na}:P_K) was approximately 10:1 for wild-type αbENaC, which fell to 2:1 and 3:1 for K504E and K515E αbENaC, respectively.

mental data to the first-order Michealis-Menten equation (Eq. 1). Furthermore, the K_m values determined from these plots also differed between channels (29.5 ± 4.2 μM, 24.3 ± 4.1 μM, and 25.4 ± 3.5 μM for wild-type (n = 3), K515E αbENaC (n = 3), and K504E αbENaC (n = 3), respectively). Therefore, the residue changes introduced into αbENaC at positions 504 and 515 affect the P_{Na}:P_K selectivity ratio because of increases in the affinity and conductance of the channel for K^+.

Inhibition of K504E and K515E αbENaC by amiloride

One of the defining characteristics of the ENaC family of Na^+ channels is their sensitivity to the K^+ sparing diuretic amiloride. Low concentrations of amiloride (0.1–0.2 μM) caused a block of the wild-type channel, with a dramatic change in the time constants for both the open and closed states, as revealed by dwell-time histogram analysis (Fig. 5). A further increase in the amiloride concentration (although still in the submicromolar range) reduced the P_o nearly to zero. The apparent inhibitory equilibrium dissociation constant (K_i) for amiloride under these conditions was 0.11 ± 0.03 μM (n = 12). Both K504E and K515E αbENaC were sensitive to amiloride and exhibited a similar pattern of response, i.e., a dramatic increase in channel closed time and a decrease in open time in the presence of amiloride (Figs. 6 and 7). However, although still responsive to amiloride, the sensitivity of the mutated αbENaC channels to this drug was shifted to the right (Fig. 8). Under these conditions, the K_i' was 0.54 ± 0.10 μM for amiloride of K515E αbENaC (n = 6) and 0.95 ± 0.18 μM for K504E αbENaC (n = 7). These observations strongly suggest that residues and/or regions in the channel, in addition to those previously thought to interact with amiloride, may also influence the sensitivity of the αENaCs to this blocker.

The basic Neher-Steinbach model proposed for a slow block of an ion channel is

$$\text{Closed} \underset{\beta}{\overset{\alpha}{\rightleftharpoons}} \text{Open} \underset{k_{off}}{\overset{k_{on}}{\rightleftharpoons}} \text{Blocked}, \qquad (2)$$

where α and β are the rate constants for the drug-independent one-step channel gating reaction, and k_{on} and k_{off} are the rate constants for binding and unbinding of the inhibitor (Neher and Steinbach, 1978). The open and closed time histograms for αbENaC in the absence of inhibitor were well described by a single exponential equation,

$$y = a \cdot \exp(-x/\tau), \qquad (3)$$

where x is the number of events within a certain time range, a is the maximum of the experimental function, and τ is the time constant. In the presence of amiloride, a second exponential component appeared (see amplitude histograms). Therefore, these data were fitted to a double exponential

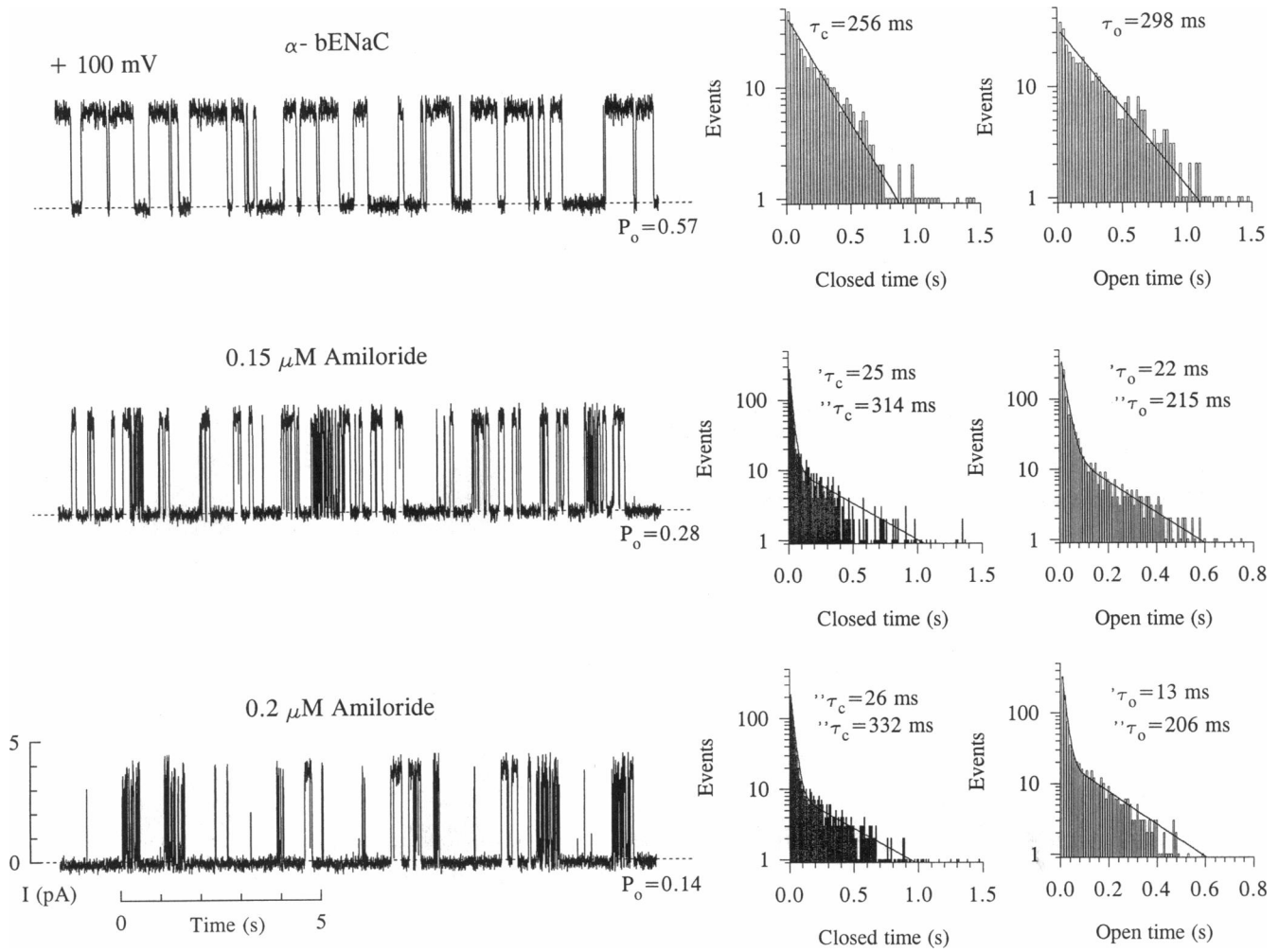

FIGURE 5 Effect of amiloride on wild-type αbENaC. The K^+ sparing diuretic amiloride caused a dose-dependent reduction in single-channel open probability of wild-type αbENaC. Low concentrations of amiloride caused an initial fast block of the channel, as manifested by a dramatic reduction in the time constants for both the open and closed states. Higher concentrations of the diuretic were associated with an increase in τ_c to more than twice the control value. Similarly, τ_o was reduced to one-tenth of the control value. Single-channel analog data were filtered at 300 Hz, using an 8-pole Bessel filter before acquisition, and were sampled at 1000 Hz, using a Digidata 1200 interface. The records shown were subsequently digitally filtered at 100 Hz using pCLAMP software, and represent appropriate sections of continuous recording while increasing amiloride concentrations in 12 separate experiments. Associated single-channel open and closed time histograms were constructed by using events lists generated by pCLAMP software from the recordings within burst periods of 4–6 min in length with 50% amplitude detection threshold and 5 ms duration threshold. The τ_c and τ_o values were calculated from double exponential fits for closed and open states, respectively. The histograms shown were constructed from 392, 1134, and 916 events for control and 0.15 μM and 0.2 μM of amiloride, respectively. In the absence of amiloride, counts were binned with a 25-ms bin width, and in the presence of amiloride with a 10-ms bin width. The holding potential was +100 mV. Dashed lines represent the zero current level.

function,

$$y = a_1 \cdot \exp(-x/\tau_1) + a_2 \cdot \exp(-x/\tau_2). \quad (4)$$

The observation of a double-exponentially distributed open time does not agree with the above proposed model of open channel block by amiloride. To accommodate these findings, the model can be modified to allow two open states:

$$\text{Closed} \underset{\beta}{\overset{\alpha}{\rightleftharpoons}} \text{Open} \underset{k'_{off}}{\overset{k'_{on}}{\rightleftharpoons}} \text{Open} \cdot \text{Bound} \underset{k''_{off}}{\overset{k''_{on}}{\rightleftharpoons}} \text{Blocked}, \quad (5)$$

or, alternatively,

$$\begin{array}{ccccc} \text{Closed} & \underset{\beta}{\overset{\alpha}{\rightleftharpoons}} & \text{Open} & \underset{k'_{off}}{\overset{k'_{on}}{\rightleftharpoons}} & \text{Blocked} \\ & & k''_{on} \uparrow\downarrow k''_{off} & & \\ & & \text{Open} \cdot \text{Bound} & & \end{array} \quad (6)$$

The Open · Amiloride Bound state is different from the Open state in that the channel can still conduct ions, even though amiloride is bound. However, the second exponent in the open time histograms was evident only at low amiloride concentrations (≤0.2 μM for WT and ≤1 μM for the

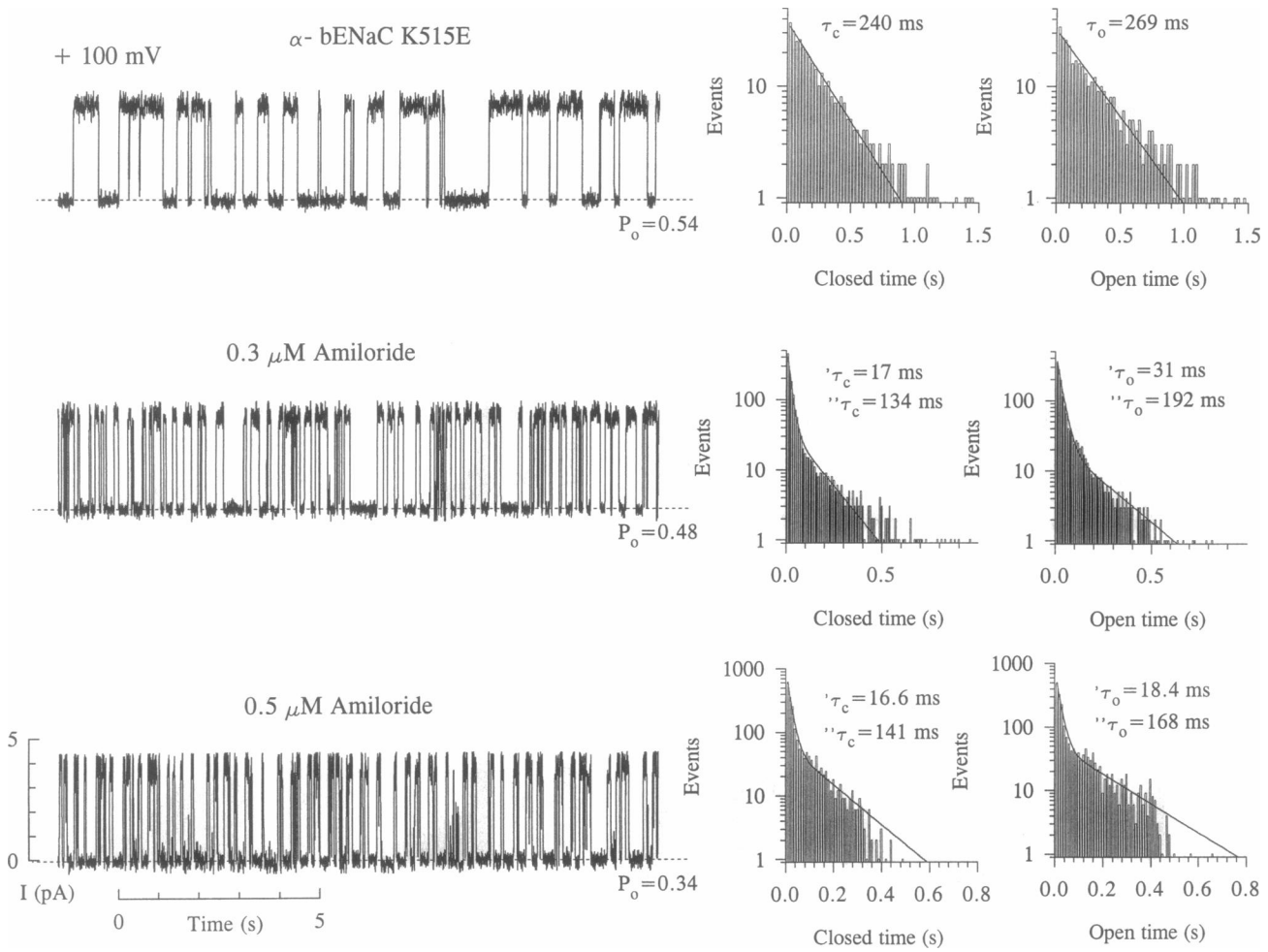

FIGURE 6 Effect of amiloride on K504E αbENaC. The point mutation K504E was also sensitive to amiloride and gave a pattern of response to the drug similar to that of the wild-type channel, in that low concentrations of amiloride were associated with an initial fast block, as evidenced by an initial fall in the values for both τ_o and τ_c. Higher concentrations of amiloride were associated with an increase in τ_c, and a corresponding decrease in τ_o. However, the concentration at which amiloride was effective was increased by an order of magnitude, as compared to the wild-type channel. Thus amiloride was a much less effective blocker of K504E αbENaC than it was of the wild-type channel. Each record is representative of seven separate experiments. In all experiments, amiloride was effective from the *trans* side of the bilayer only. Single-channel analog data were filtered at 300 Hz using an 8-pole Bessel filter before acquisition, and were sampled at 1000 Hz using a Digidata 1200 interface. Records shown were subsequently digitally filtered at 100 Hz using pCLAMP software and represent sections of continuous recordings with increasing amiloride concentrations. Associated single-channel open and closed time histograms were constructed using events lists generated by pCLAMP software from the recordings within burst periods of 4–6 min in length, with 50% amplitude detection threshold and 5-ms duration threshold. Single-channel open and closed time histograms were constructed from 394, 791, and 1973 events for control and 0.3 μM and 1 μM amiloride, respectively. Binning was the same as indicated for the histograms in Fig. 3. The τ_c and τ_o values were calculated from double exponential fits for closed and open states, respectively. The holding potential was +100 mV. Dashed lines represent zero current levels.

mutants). The absence of the second open state at higher amiloride concentrations may mean that at these concentrations the most favorable blocking mechanism is an open-channel block. Our conclusions are consistent with the observation of two closed states and one open state in the native channel in A6 cells (reported at 0.5 μM amiloride; Hamilton and Eaton, 1985). Palmer and Frindt (1986a,b) also reported one closed state and one open state for amiloride block of the channel in rat cortical collecting tubule, at 0.5 μM and 1 μM amiloride, respectively. The assumption that amiloride can bind to the open state of the channel without blocking the conduction pathway is consistent with the hypothesis that epithelial Na^+ channels have multiple binding sites for amiloride. The shorter time constants in the open state, but not in the closed states, were amiloride concentration dependent (Fig. 9). Based on the above assumptions, we have calculated the blocking (k_{on}) and unblocking (k_{off}) rate constants for amiloride as inverse values of the shorter time constants in both open and closed states. Evident from the analyses was the finding that both charge mutations of αbENaC decrease k_{on} and increase k_{off} for amiloride. The ratios of these constants yield dissociation

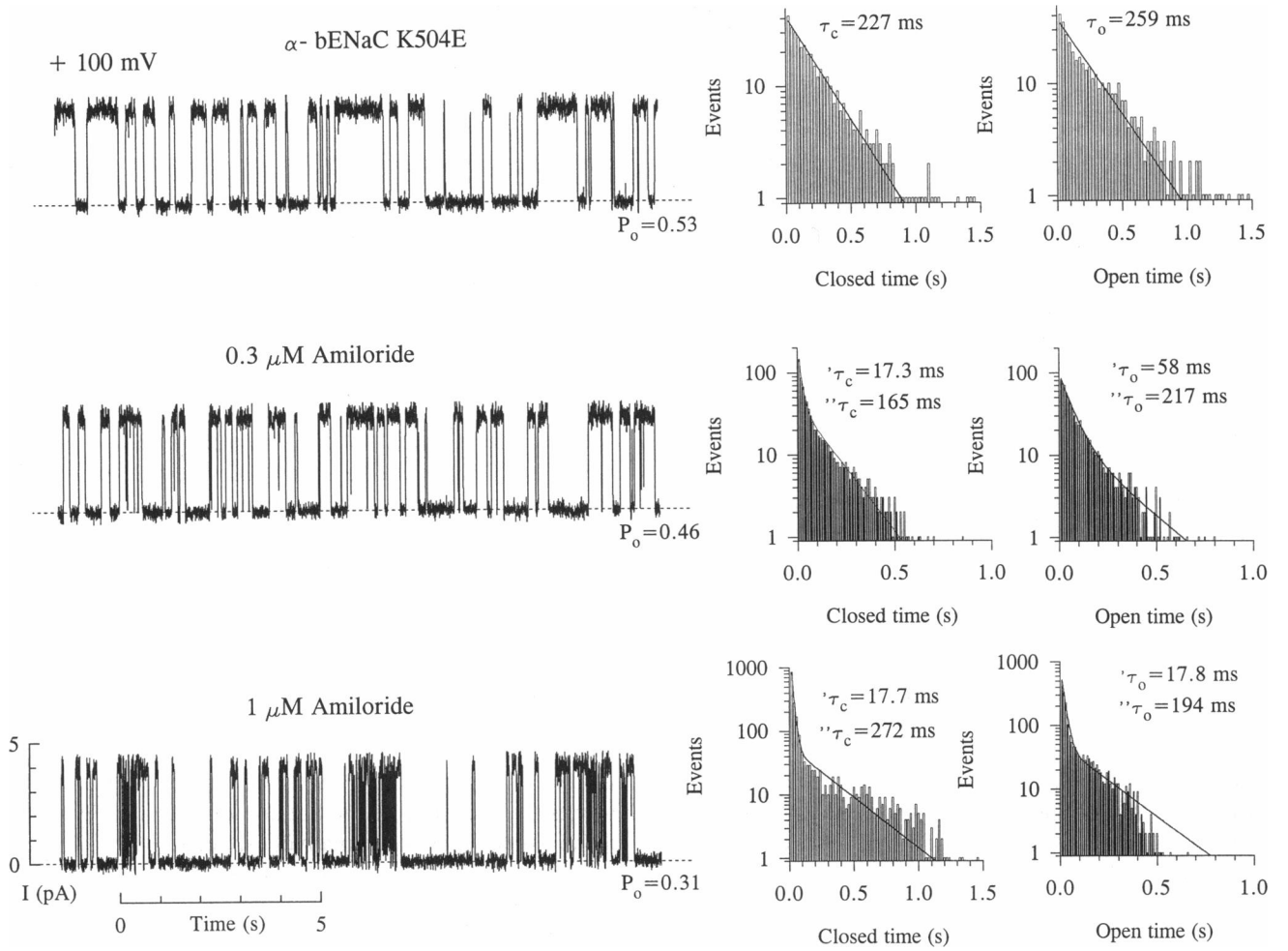

FIGURE 7 Effect of amiloride on K515E αbENaC. As with the effect of amiloride on K504E αbENaC, K515E αbENaC required a concentration of amiloride an order of magnitude greater than that required to inhibit the wild-type channel to the same extent. However, the responses of this mutant were nearly identical to those of K504E αbENaC in that there was an initial fast block of the channel at lower amiloride concentrations with an associated increase in τ_c, and a corresponding decrease in τ_o at higher concentrations. Each record is representative of six separate experiments. In all experiments, amiloride was effective from the *trans* side of the bilayer only. Single-channel analog data were filtered at 300 Hz, using an 8-pole Bessel filter before acquisition, and were sampled at 1000 Hz, using a Digidata 1200 interface. Records shown were subsequently digitally filtered at 100 Hz using pCLAMP software and represent typical sections of continuous recording while amiloride concentrations are increased. Associated single-channel open and closed time histograms were constructed using events lists generated by pCLAMP software from the recordings within burst periods of 4–6 min in length with 50% amplitude detection threshold and 5-ms duration threshold. Single-channel open and closed time histograms were constructed from 363, 1523, and 1997 events for control and 0.3 μM and 0.5 μM amiloride, respectively. The τ_c and τ_o values were calculated from double-exponential fits for closed and open states, respectively. Binning was the same as indicated for the histograms in Fig. 3. The holding potential was +100 mV. Dashed lines represent zero current levels.

constant (K_d) values for amiloride of 0.13, 0.55, and 1.06 μM for wild-type, K515E, and K504E, respectively. These K_d values are close to those determined from dose-response curves (cf. Fig. 8). The longer time constants in the open time histograms disappear with increasing amiloride concentration, thus making it impossible to test the proposed model further.

DISCUSSION

Identification of functional domains in the primary sequence of a channel is a fundamental step in the elucidation of channel characteristics and mechanisms of action. The observation that the αENaC subunit can act as a channel in its own right (although the addition of the nonconductive β and γ subunits serves to augment the magnitude of the total amiloride-sensitive current) suggests that αENaC has a primary role in the formation of the channel pore. In several cation channels, the amino acids arginine and lysine form a site for fixed positive charges in the channel's primary structure that are then available to interact with either the conducted moiety or other portions of the channel protein (Perozo et al., 1994; Kienker et al., 1994). In the present study we have generated single point mutations in a lysine-rich region of the putative external loop of the αbENaC Na^+ channel. We hypothesized that mutations in this region

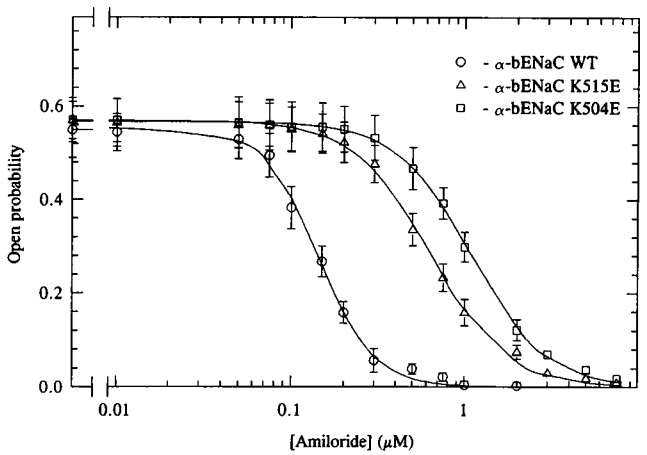

FIGURE 8 Summary of amiloride dose-response curves for wild type, K504E, and K515E αbENaC. Although all three channels were sensitive to amiloride, both K504E and K515E had much attenuated responses to the drug, with K515E being slightly less sensitive than K504E. These data suggest that more than a single region in αbENaC may influence the interaction of amiloride with this family of epithelial Na^+ channels.

might lead to alterations in channel conductance, as occurs when similar mutations are constructed in the nicotinic acetylcholine receptor channel (Kienker et al., 1994). Although we did not detect any change in the single-channel conductance of αbENaC, we did observe that the two mutations constructed, K504E and K515E, evoked dramatic changes in the channel's kinetic fingerprint.

Both mutations caused an obvious change in the gating pattern of the wild-type channel, which is normally characterized by a pronounced bursting activity. Whereas K515E increased the frequency of the bursts, in the K504E mutant the burst pattern was completely eradicated, with the overall open probability of the channel markedly increasing. We have previously observed a similar phenomenon upon truncation of a portion of the C terminal of αbENaC (Fuller et al., 1996). In the αbENaC truncation mutant αbENaC R567X, the bursting of channel activity was abolished, and instead of the channel exhibiting a single-step transition to 39 pS, it exhibited two steps, an almost constitutively open 13-pS state, in addition to which was seen a second step of 26 pS. This pattern was identical to what was observed when wild-type αrENaC was incorporated into the lipid bilayer (Fuller et al., 1996; Ismailov et al., 1996a). In the region of αbENaC mutated in the present series of experiments, the homology between αbENaC and αrENaC is nearly 100%. However, the observation that the lack of a burst-type gating pattern of K504E αbENaC was very similar to that seen for wild-type αrENaC and for the αbENaC truncation mutant R567X suggests that this single point mutation can compensate in part for the effects that the C terminal has on the gating of αbENaC, although neither of the present mutations had any effect on the pattern of the single step transitions. One additional difference not observed in the R567X αbENaC truncation mutant was that in both K504E and K515E αbENaC there was a significant reduction in ion selectivity (Na^+:K^+) of the channel, which fell by approximately three- to fivefold.

The gating pattern was not the only parameter affected by the two point mutations. Sensitivity to the diuretic amiloride is one of the key features of the ENaC family of Na^+ channels, and amiloride is just as effective a blocker of conduction through channels formed by αENaC alone as it is of the αβγENaC complex. The affinity of this family of channels for the blocker is extremely high, with K_i' values in the submicromolar range when studied under single-channel conditions (Ismailov et al., 1995). The site of action of this blocker is known to lie at the external surface of the channel (Kleyman and Cragoe, 1988; Benos, 1988); for ENaC in the lipid bilayer system, amiloride is effective only from one side (Ismailov et al., 1995). Correspondingly, a putative amiloride-binding site has been identified in the external loop region of the αrENaC subunit, comprising residues 278–283, a region that is highly conserved across all αENaC subunits identified to date. Deletion of this region shifts the K_i' by two orders of magnitude (Ismailov et al., manuscript submitted for publication). However, when we examined the sensitivity to amiloride of K504E αbENaC and K515E αbENaC, we found that both of these mutations had much lower affinities for amiloride than did the wild-type channel, even though sequence analysis revealed no mutations in the putative amiloride-binding domain. These results are in contrast to the findings of Li et al. (1995), who demonstrated that an alternatively spliced form of αrENaC, (αrENaCa), which lacks the last 199 amino acids of the wild-type αrENaC sequence, exhibited no difference in the ability of either the amiloride analog phenamil, or amiloride itself, to displace [^{3}H]phenamil bound to cells heterologously expressing αrENaCa. However, expression of this splice variant, which lacks both the second transmembrane domain and the lysine-rich region mutated in the present study, was not associated with expression of an appreciable amiloride-sensitive Na^+ current. However, the present results suggest that the lysine-rich region preceding M2 may also be involved in the external block of the channel with amiloride. The detailed mechanism of how the replacement of distant fixed charges at the putative outer mouth of the αbENaC pore affects amiloride binding remains unknown. Both mean open and closed times of the wild-type channel and mutant channels are in agreement with the reduction of mean open time and the increase in mean closed time found with increasing amiloride concentration that was observed in earlier measurements of single amiloride-sensitive Na^+ channels in A6 cells and rat cortical collecting tubules (Hamilton and Eaton, 1985; Palmer and Frindt, 1986a,b). The role of the β and γENaC subunits in amiloride binding to this Na^+ channel also remains to be determined, although previous experiments did not reveal any difference in amiloride sensitivity of the channels formed by the α subunit of the originally cloned rat epithelial Na^+ channel alone, and that of heterologously expressed α, β, γ-rENaC.

In summary, we have shown that a region immediately before the second transmembrane domain of αbENaC may

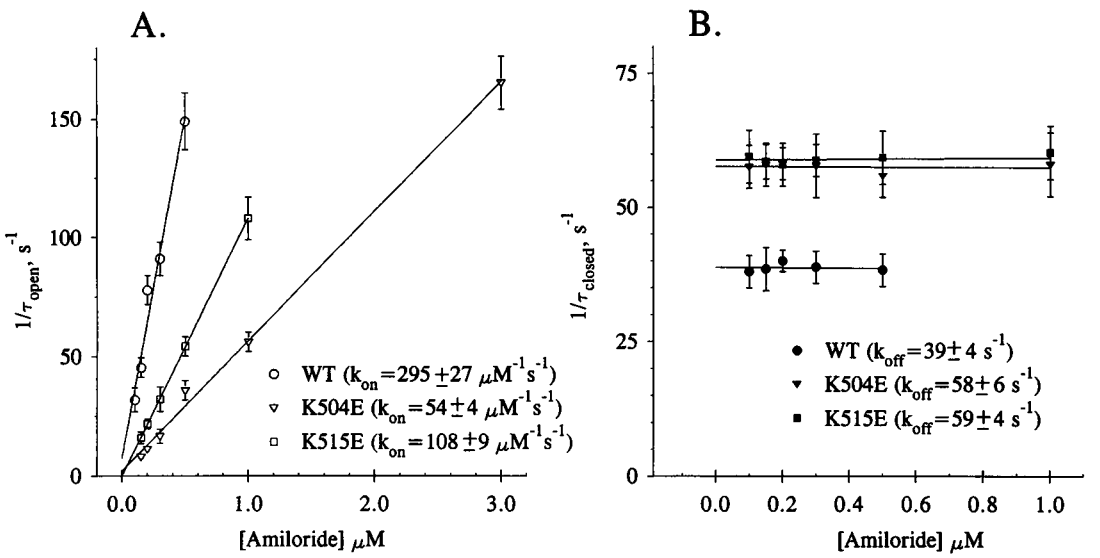

FIGURE 9 Reciprocal plots of τ_o (*A*) and τ_c (*B*) versus amiloride concentration for wild type (WT), K515E, and K504E αbENaC. Data points and error bars represent the mean ± 1 SD for at least six separate experiments at each amiloride concentration. Lines in the graphs represent first-order regression of the data. The blocking rate constants (k_{on}) for amiloride were calculated as 295 ± 27 μM^{-1} s^{-1} for wild-type αbENaC and 108 ± 9 μM^{-1} s^{-1} and 54 ± 4 μM^{-1} s^{-1} for K515E and K504E αbENaC, respectively. Unblocking rate constants were calculated as 39 ± 4, 59 ± 4, and 58 ± 6 for wild type (n = 9), K515E (n = 7), and K504E (n = 6) αbENaC, respectively.

have an important role in the regulation of fundamental channel properties such as gating kinetics, ion selectivity, and amiloride sensitivity. In particular, the location of fixed positive charges on lysine residues in this region seems to be important to the maintenance of channel characteristics. Furthermore, we have demonstrated that the extracellular loop has a significant role in the structure/function-based regulation of the ENaC channels. The regulation of the ENaCs is likely to be highly complex, as more than a single site appears to be involved in determining amiloride binding and patterns of gating. Site-directed mutagenesis will be a useful tool in further studies to determine functional sites in the ENaC channel proteins.

We would like to thank Christie Browne for excellent assistance with the expression of ENaC cRNAs in *Xenopus* oocytes, and Elizabeth Fernandez for superb technical assistance.

This study was supported by National Institutes of Health grant DK37206.

REFERENCES

Awayda, M. S., I. I. Ismailov, B. K. Berdiev, and D. J. Benos. 1995. A cloned epithelial Na^+ channel protein displays stretch activation in planar lipid bilayers. *Am. J. Physiol.* 268:C1450–C1459.

Benos, D. J. 1988. Amiloride: chemistry, kinetics and structure-activity relationships. *In* Na^+/H^+ Exchange. S. Grinstein, editor. CRC Uniscience, Boca Raton, FL. 121–136.

Bubien, J. K., I. I. Ismailov, B. K. Berdiev, T. Cornwell, R. P. Lifton, C. M. Fuller, J.-M. Achard, D. J. Benos, and D. G. Warnock. 1996. Liddle's disease: abnormal regulation of amiloride-sensitive Na^+ channels by β-subunit mutation. *Am. J. Physiol.* 270:C208–C213.

Canessa, C. M., J.-D. Horisberger, and B. C. Rossier. 1993. Epithelial sodium channel related to proteins involved in neurodegeneration. *Nature.* 361:467–470.

Canessa, C. M., A. M. Merillat, and B. C. Rossier. 1994a. Membrane topology of the epithelial sodium channel in intact cells. *Am. J. Physiol.* 267:C1682–C1690.

Canessa, C. M., L. Schild, G. Buell, B. Thorens, I. Gautschi, J. D. Horisberger, and B. C. Rossier. 1994b. Amiloride-sensitive epithelial Na^+ channel is made of three homologous subunits. *Nature.* 367: 463–467.

Chalfie, M., and E. Wolinsky. 1990. The identification and suppression of inherited neurodegeneration in *Caenorhabditis elegans. Nature.* 345: 410–416.

Chang, S. S., S. Grunder, A. Hanukoglu, A. Rosler, P. M. Mathew, I. Hanukoglu, L. Schild, Y. Lu, R. A. Shimkets, C. Nelson-Williams, B. C. Rossier, and R. P. Lifton. 1996. Mutations in subunits of the epithelial sodium channel cause salt wasting with hyperkalaemic acidosis, pseudohypoaldosteronism type 1. *Nature Genet.* 12:248–253.

Cunningham, S. A., M. S. Awayda, J. K. Bubien, I. I. Ismailov, M. P. Arrate, B. K. Berdiev, D. J. Benos, and C. M. Fuller 1995. Cloning of an epithelial chloride channel from bovine trachea. *J. Biol. Chem.* 270: 31016–31026.

Driscoll, M., and M. Chalfie. 1991. The mec-4 gene is a member of a family of *Caenorhabditis elegans* genes that can mutate to induce neuronal degeneration. *Nature.* 349:588–593.

Fuller, C. M., M. S. Awayda, M. P. Arrate, A. L. Bradford, R. G. Morris, C. M. Canessa, B. C. Rossier, and D. J. Benos. 1995. Cloning of a bovine renal epithelial Na^+ channel subunit. *Am. J. Physiol.* 269: C641–C654.

Fuller, C. M., I. I. Ismailov, B. K. Berdiev, V. G. Shlyonsky, and D. J. Benos. 1996. Kinetic interconversion of rat and bovine homologs of the α subunit of an amiloride-sensitive Na^+ channel by C-terminal truncation of the bovine subunit. *J. Biol. Chem.* 271:26602–26608.

Hamilton, K. L., and D. C. Eaton. 1985. Single-channel recordings from amiloride-sensitive epithelial sodium channels. *Am. J. Physiol.* 249: C200–C207.

Hansson, J. H., C. Nelson-Williams, H. Suzuki, L. Schild, R. Shimkets, Y. Lu, C. Canessa, T. Iwasaki, B. Rossier, and R. P. Lifton. 1995a. Hypertension caused by a truncated epithelial sodium channel γ subunit: genetic heterogeneity of Liddle syndrome. *Nature Genet.* 11:76–82.

Hansson, J. H., L. Schild, Y. Lu, T. A. Wilson, I. Gautschi, R. Shimkets, C. Nelson-Williams, B. C. Rossier, and R. P. Lifton. 1995b. A de novo

missense mutation of the β subunit of the epithelial sodium channel causes hypertension and Liddle syndrome, identifying a proline-rich segment critical for regulation of channel activity. *Proc. Natl. Acad. Sci. USA.* 92:11495–11499.

Hoshi, T., W. N. Zagotta, and R. W. Aldrich. 1990. Biophysical and molecular mechanisms of *Shaker* potassium channel inactivation. *Science.* 250:533–538.

Imoto, K., C. Busch, B. Sakmann, M. Mishina, T. Konno, J. Nakai, H. Bujo, Y. Mori, K. Fukuda, and S. Numa. 1988. Rings of negatively charged amino acids determine the acetylcholine receptor channel conductance. *Nature.* 335:645–648.

Ismailov, I. I., M. S. Awayda, B. K. Berdiev, J. K. Bubien, J. E. Lucas, C. M. Fuller, and D. J. Benos. 1996a. Triple-barrel organization of ENaC, a cloned epithelial Na^+ channel. *J. Biol. Chem.* 271:807–816.

Ismailov, I. I., B. K. Berdiev, and D. J. Benos. 1995. Biochemical status of renal epithelial Na^+ channels determines apparent channel conductance, ion selectivity, and amiloride sensitivity. *Biophys. J.* 69:1789–1800.

Ismailov, I. I., B. K. Berdiev, C. M. Fuller, A. L. Bradford, R. P. Lifton, D. G. Warnock, J. K. Bubien, and D. J. Benos. 1996b. Peptide block of constitutively activated Na^+ channels in Liddle's disease. *Am. J. Physiol.* 270:C214–C223.

Kienker, P., G. Tomaselli, M. Jurman, and G. Yellen. 1994. Conductance mutations of the nicotinic acetylcholine receptor do not act by a simple electrostatic mechanism. *Biophys. J.* 66:325–334.

Kleyman, T. R., and E. J. Cragoe, Jr. 1988. Amiloride and its analogs as tools in the study of ion transport. *J. Membr. Biol.* 105:1–21.

Konno, T., C. Busch, E. von Kitzing, K. Imoto, F. Wang, J. Nakai, M. Mishina, S. Numa, and B. Sakmann. 1991. Rings of anionic amino acids as structural determinants of ion selectivity in the acetylcholine receptor channel. *Proc. R. Soc. Lond. Biol.* 244:69–79.

Lakshminarayanaiah, N. 1984. Equations of Membrane Biophysics. Academic Press, Orlando, FL.

Li, X.-J., R.-H. Xu, W. B. Guggino, and S. H. Snyder. 1995. Alternatively spliced forms of the α subunit of the epithelial sodium channel: distinct sites for amiloride binding and channel pore. *Mol. Pharmacol.* 47: 1133–1140.

Lingueglia, E., G. Champigny, M. Lazdunski, and P. Barbry. 1995. Cloning of the amiloride-sensitive FMRFamide peptide-gated sodium channel. *Nature.* 378:730–733.

Lingueglia, E., N. Voilley, R. Waldman, M. Lazdunski, and P. Barbry. 1993. Expression cloning of an epithelial amiloride-sensitive Na^+ channel. A new channel type with homologies to *Caenorhabditis elegans* degenerins. *FEBS Lett.* 318:95–99

MacKinnon, R., and C. Miller. 1989. Functional modification of a Ca^{2+}-activated K^+ channel by trimethyloxonium. *Biochemistry.* 28: 8087–8092.

McDonald, F. J., M. P. Price, P. M. Snyder, and M. J. Welsh. 1995. Cloning and expression of the β- and γ-subunits of the human epithelial sodium channel. *Am. J. Physiol.* 268:C1157–C1163.

McDonald, F. J., and M. J. Welsh. 1995. Binding of the proline-rich region of the epithelial Na^+ channel to SH3 domains and its association with specific cellular proteins. *Biochem. J.* 312:491–497.

McDonald, F. J., P. M. Snyder, P. B. McCray, Jr., and M. J. Welsh. 1994. Cloning, expression and tissue distribution of a human amiloride-sensitive Na^+ channel. *Am. J. Physiol.* 266:L728–L734.

Neher, E., and J. H. Steinbach, 1978. Local anaesthetics transiently block currents through single acetylcholine-receptor channels. *J. Physiol. (Lond.).* 277:153–176.

Palmer, L. G., and G. Frindt. 1986a. Epithelial sodium channels: characterization by using the patch-clamp technique. *Fed. Proc.* 45: 2708–2712.

Palmer, L. G., and G. Frindt. 1986b. Amiloride-sensitive Na^+ channels from the apical membrane of the rat cortical collecting tubule. *Proc. Natl. Acad. Sci. USA.* 83:2767–2770.

Perez, G., A. Lagrutta, J. P. Adelman, and L. Toro. 1994. Reconstitution of expressed K_{Ca} channels from *Xenopus* oocytes to lipid bilayers. *Biophys. J.* 66:1022–1027.

Perozo, E., L. Santacruz-Toloza, E. Stefani, F. Bezanilla, and D. M. Papazian. 1994. S4 mutations alter gating currents of Shaker K channels. *Biophys. J.* 66:345–354.

Price, M. P., P. M. Snyder, and M. J. Welsh. 1996. Cloning and expression of a novel human brain Na^+ channel. *J. Biol. Chem.* 271:7879–7882.

Renard, S., E. Lingueglia, N. Voilley, M. Lazdunski, and P. Barbry. 1994. Biochemical analysis of the membrane topology of the amiloride sensitive Na^+ channel. *J. Biol. Chem.* 269:12981–12986.

Rotin, D., D. Bar-Sagi, H. O'Brodovich, J. Merlainen, P. V. Lehto, C. M. Canessa, B. C. Rossier, and G. P. Downey. 1994. A SH3 binding region in the epithelial Na^+ channel (αrENaC) mediates its localization at the apical membrane. *EMBO J.* 13:4440–4450.

Schild, L., Y. Lu, I. Gautschi, E. Schneeberger, R. P. Lifton, and B. C. Rossier. 1996. Identification of a PY motif in the epithelial Na channel subunits as a target sequence for mutations causing channel activation found in Liddle syndrome. *EMBO J.* 15:2381–2387.

Shimkets, R. A., D. G. Warnock, C. M. Bositis, C. Nelson-Williams, J. H. Hansson, M. Schambelan, J. R. J. Gills, S. Ulick, R. V. Milora, J. W. Findling, C. M. Canessa, B. C. Rossier, and R. P. Lifton. 1994. Liddle's syndrome: inheritable human hypertension caused by mutations in the β subunit of the epithelial sodium channel. *Cell.* 79:407–414.

Snyder, P. M., F. J. McDonald, J. B. Stokes, and M. J. Welsh. 1994. Membrane topology of the amiloride-sensitive epithelial sodium channel. *J. Biol. Chem.* 269:24379–24383.

Staub, O., S. Dho, P. C. Henry, J. Correa, T. Ishikawa, J. McGlade, and D. Rotin. 1996. WW domains of Nedd4 bind to the proline-rich PY motifs in the epithelial Na^+ channel deleted in Liddle's syndrome. *EMBO J.* 15:2371–2380.

Voilley, N., F. Bassilana, C. Mignon, S. Merscher, M. G. Mattei, G. F. Carle, M. Lazdunski, and P. Barbry. 1995. Cloning, chromosomal localization, and physical linkage of the beta and gamma subunits (SCNN1B and SCNN1G) of the human epithelial amiloride-sensitive sodium channel. *Genomics.* 28:560–565.

Voilley, N., E. Lingueglia, G. Champigny, M. G. Mattei, R. Waldmann, M. Lazdunski, and P. Barbry. 1994. The lung amiloride sensitive Na^+ channel: biophysical properties, pharmacology, ontogenesis and molecular cloning. *Proc. Natl. Acad. Sci. USA.* 91:247–251.

Worley, J. F., III, R. J. French, and B. K. Krueger. 1986. Trimethyloxonium modification of single batrachotoxin-activated sodium channels in planar bilayers. *J. Gen. Physiol.* 87:327–349.

Zagotta, W. N., T. Hoshi, and R. W. Aldrich. 1990. Restoration of inactivation of mutants of *Shaker* potassium channels by a peptide derived from ShB. *Science.* 250:568–571.